Journal of Magnetic Resonance 214 (2012) 281–288

Contents lists available at SciVerse ScienceDirect

Journal of Magnetic Resonance

journal homepage: www.elsevier.com/locate/jmr

Emulsion droplet sizing using low-field NMR with chemical shift resolution and the block gradient pulse method

I.A. Lingwood [a], T.C. Chandrasekera [a], J. Kolz [a], E.O. Fridjonsson [b], M.L. Johns [b,*]

[a] Department of Chemical Engineering and Biotechnology, University of Cambridge, Pembroke Street, Cambridge CB23RA, UK
[b] School of Mechanical and Chemical Engineering, University of Western Australia, 35 Stirling Highway, Crawley WA 6009, Australia

ARTICLE INFO

Article history:
Received 9 September 2011
Revised 24 November 2011
Available online 8 December 2011

Keywords:
Emulsions
PFG
Micro-coils
Chemical shift
Bench-top spectrometer

ABSTRACT

Pulsed Field Gradient (PFG) measurements are commonly used to determine emulsion droplet size distributions based on restricted self-diffusion within the emulsion droplets. Such measurement capability is readily available on commercial NMR bench-top apparatus. A significant limitation is the requirement to selectively detect signal from the liquid phase within the emulsion droplets; this is currently achieved using either relaxation or self-diffusion contrast. Here we demonstrate the use of a 1.1 T bench-top NMR magnet, which when coupled with an rf micro-coil, is able to provide sufficient chemical shift resolution such that unambiguous signal selection is achieved from the dispersed droplet phase. We also improve the accuracy of the numerical inversion process required to produce the emulsion droplet size distribution, by employing the Block Gradient Pulse (bgp) method, which partially relaxes the assumptions of a Gaussian phase distribution or infinitely short gradient pulse application inherent in current application. The techniques are successfully applied to size 3 different emulsions.

1. Introduction

Emulsions are liquid dispersions of one immiscible droplet phase within another continuous phase. They are frequently encountered in a wide range of industrial contexts ranging from foodstuffs [1] to oilfield emulsions [2]. An essential characteristic is their droplet size distributions (typically in the 1–10 μm range) which can determine, for example, microbial stability [3], rheological properties [4,5] and physical stability and hence shelf-life [6]. Hence accurate measurement of this droplet size distribution is an essential metrology need. Originally proposed and developed by several research groups [7–9], the use of Pulsed Field Gradient (PFG) NMR to measure emulsion droplet size distributions has become a viable measurement option commercially available as part of various bench-top NMR apparatus. Advantages of this approach include an ability to readily be applied to opaque and/or concentrated emulsion systems and to sample a comparatively larger sample volume, relative to optical techniques for example. Several reviews [10,11] of this NMR emulsion characterisation technique are available in the literature.

The technique also features several disadvantages relative to its competitors; primarily these are a limited accessible droplet size range (due to the requirement that diffusion be sufficiently restricted in the droplets coupled with a limited diffusion time dictated by T_1 relaxation) and cost. Cost is partially addressed by application on bench-top NMR apparatus typically operating at magnetic field strengths of 0.05–1 T [11]. One of the first implementations of PFG NMR for emulsion droplet sizing using bench-top NMR was performed by Fourel et al. [12], whilst the first measurements on warer-in-oil emulsions were reported by van den Eden [13]. The droplet sizes of butter emulsions were successfully determined using a Bruker minispec pc120 operating at 20 MHz; the results were comparable to those obtained by other methods. Goudappel et al. [14] similarly used a bench-top NMR system to acquire droplet size distributions of oil–water food emulsions, suppression of the continuous phase signal was achieved using diffusion editing. Denkova et al. [15] made use of diffusion weighting to remove the unwanted continuous water phase signal whilst using a Bruker Minspec MQ20 (20 MHz) bench-top system to determine the droplet size distributions for a variety of soybean oil-in-water emulsions. Though the distribution of sizes were 20% smaller than expected, no systematic error was evident and the precision of the results was comparable to the other methods. van Duynhoven et al. [16] confirmed the applicability of PFG NMR for obtaining droplet size distributions at low field by comparing such DSD's for a number of oil-in-water and water-in-oil emulsions to those obtained by laser scattering, electrical sensing and confocal scanning laser microscopy. By combining a CPMG pre-encode with a PFG pulse sequence, Pena and Hirsaki [17] were able to obtain phase differentiation of water-in-crude oil emulsions using a 2.3 MHz bench-top system.

* Corresponding author.
E-mail address: michael.johns@uwa.edu.au (M.L. Johns).

1090-7807/$ - see front matter © 2011 Elsevier Inc. All rights reserved.
doi:10.1016/j.jmr.2011.11.020

More recently Bot et al. [18] used a 20 MHz Bruker minispec Q20 to verify droplet structure and size distributions in temperature-cycled oil-in-water emulsions. A comprehensive review of the use of bench-top NMR for the determination of droplet size distributions is given by Voda and van Duynhoven [1] and van Duynhoven et al. [19].

Currently for such bench-top measurements, selective detection of the droplet phase signal for PFG analysis is achieved by exploiting T_1 relaxation (e.g. [16]) or diffusion (e.g. [14]) contrast between the droplet phase and the continuous phase to effectively weight out the contribution from the continuous phase. Such methodology is not unambiguous as prior knowledge is required as to whether complete continuous phase signal suppression has been achieved, significant differences are required in the respective diffusion or T_1 relaxation parameters of the droplet and continuous phases respectively and achievable signal-to-noise ratios (SNRs) are also generally reduced via use of these suppression methods. In the case of using T_1 relaxation or nulling to eliminate the oil signal from water-in-oil emulsions (e.g. water-in-crude oil emulsions), an explicit requirement is that the oil system present a single value of T_1, this is often not the case. Clearly it would be desirable to employ chemical shift differentiation of the continuous and droplet phases, this would be unambiguous and optimise the available SNR. The required magnetic field homogeneity is however not readily available on bench-top apparatus [20].

Our work reported here presents two new features which improve on current bench-top NMR emulsion droplet sizing: First we demonstrate that via the use of a bench-top 1.1 T magnet, an accompanying spectrometer and an appropriate radio-frequency micro-coil, we are able to adequately retain chemical shift differentiation of the droplet and continuous phase in a range of emulsions, such that emulsion droplet sizing is possible. We also improve the numerical data inversion of the acquired attenuation data, as is required to produce a droplet size distribution, by the use of the Block Gradient Pulse (bgp) method [as detailed in [21–23]], that minimises the effect of current assumptions of a Gaussian phase distribution for the acquired PFG signal or an infinitely short gradient application.

2. Background

The measurement of self-diffusion using PFG NMR was first demonstrated by Stejskal and Tanner [24]. The random motion of liquid molecules between two external magnetic field gradients causes signal (I) attenuation, which can be related to various PFG experimental parameters and the appropriate molecular coefficient of self-diffusion, D:

$$\ln\frac{I}{I_0} = -D\delta^2\gamma^2 g^2\left(\Delta - \frac{\delta}{3}\right) \tag{1}$$

Here Δ is the duration between the applied magnetic field gradients, δ is the duration for which the gradient is applied for, g is the strength of each pair of field gradients, I_0 is the signal intensity in the absence of applied magnetic field gradients and γ is the gyromagnetic ratio (2.675×10^{-8} rad s^{-1} T^{-1} for ^{1}H nuclei). Therefore, I can be measured as a function of Δ, δ or g and hence D determined. Restricted self-diffusion is experienced when geometric constraints are present such as the case of a droplet phase; the molecules within each droplet are restricted by the physical boundary between the two phases present. This results in a reduced molecular motion and hence reduced signal attenuation. In the case of restricted diffusion within spheres (as is the case for emulsions) the signal attenuation (I/I_0) can be modelled by a number of methods:

(i) The Gaussian Phase Distribution (gpd) model [8] which assumes that the NMR signal phase distribution is a Gaussian shape:

$$\frac{I}{I_0} = \exp\left[-2\gamma^2 g^2\sum_{m=1}^{\infty}\frac{1}{\alpha_m^2(\alpha_m^2a^2-2)} \times\left\{\frac{2\delta}{\alpha_m^2D} - \frac{2+e^{-\alpha_m^2D(\Delta-\delta)} - 2e^{-\alpha_m^2D\Delta} - 2e^{-\alpha_m^2D\delta} + e^{-\alpha_m^2D(\Delta+\delta)}}{(\alpha_m^2D)^2}\right\}\right] \tag{2a}$$

where α_m is given by the positive roots of the expression:

$$J_{3/2}(\alpha a) = \alpha a J_{5/2}(\alpha a), \tag{2b}$$

and where a is the droplet diameter and J_n is an nth order Bessel function.

(ii) The Short Gradient Pulse (sgp) model [36], which assumes that the duration of the applied magnetic field gradient, δ, is equal to zero, and hence there is an assumption of no self-diffusion as the gradients are applied. This leads, for a spherical geometry, to:

$$\frac{I}{I_0} = \frac{9(qa\cos(qa)-\sin(qa)^2)}{(qa)^6} + 6(qa)^2 \times\sum_{n=0}^{\infty}\left[J_n'(qa)\right]^2\sum_m\frac{(2n+1)\alpha_{nm}^2}{\alpha_{nm}^2-n^2-n}x \times\exp\left(-\frac{\alpha_{nm}^2D_0\Delta}{a^2}\right)\frac{1}{\left[\alpha_{nm}^2-(qa)^2\right]^2} \tag{3}$$

where α_{nm} is the mth root of the equation $J_n'(\alpha)=0$ and $q=\gamma\delta g$.

Both Eqs. (2) and (3) have only one free parameter, the radius of the droplets, a, all other variables are determined by experiment execution.

More recently, an improved method of describing restricted diffusion within spherical geometries has been developed. This is based on a general technique for quantifying the signal attenuation due to an arbitrary magnetic field, which results in the generalised gradient waveform set of methods (e.g. [25–27]). The attenuation within a single droplet can be obtained by solving the Bloch-Torrey equation [28] describing the magnetisation under a constant gradient phase shift vector. The solution to this form of the Bloch-Torrey equation is often intractable but can be solved by eigenfunction expansion. An expansion of the φ-averaged spatial eigenfunctions from the solution of the self-diffusion equation can be used to find a solution in the presence of a piecewise-constant gradient waveform [29]. We shall refer to this method as the Block Gradient Pulse (bgp) approximation. Details regarding the derivation can be sourced from Grebenkov [21]. The resultant expression describing signal intensity, when we divide the pulse sequence into N_e intervals of constant gradient, is given by:

$$I = \mathbf{v}^\dagger\left(\prod_{k=1}^{N_e}\mathbf{G}(\tilde{t}_k-\tilde{t}_{k-1};\tilde{\boldsymbol{\gamma}}_k)\right)\mathbf{v} \tag{4a}$$

where

$$\mathbf{G}(\tilde{t};\tilde{\boldsymbol{\gamma}}) = \exp[(-\boldsymbol{\Lambda}+i(\tilde{\boldsymbol{\gamma}}\cdot\hat{z})\mathbf{Z})\tilde{t}] \tag{4b}$$

and the elements of vector $\mathbf{v}$ are:

$$v_j = \delta_{j1} = \begin{cases}1 & j=1\\ 0 & j>1\end{cases} \tag{4c}$$

for a reflecting boundary with no surface relaxation (δ here is the Kronecker symbol). For the purpose of clarity we have made use of the following definitions:

$$\tilde{t} = \frac{D_0t}{a^2},\quad \tilde{\boldsymbol{\gamma}} = \frac{-c\gamma\mathbf{g}a^3}{D_0}\quad\text{and}\quad \Lambda_{jk} = \alpha_{nm}^2\delta_{jk} \tag{4d}$$

The matrix elements for **Z** for a sphere are given analytically by Grebenkov [21–23]. We also note that in the limit $|\tilde{\gamma}| \to 0$, **G** becomes **D**, where:

$$\mathbf{D}(\tilde{t}) = \exp[-\mathbf{\Lambda}\tilde{t}] \tag{4e}$$

After expansion of Eq. (4a) for a stimulated echo PFG pulse sequence, as used in this work and shown in Fig. 2, we can express the signal attenuation as follows:

$$\frac{I}{I_0} = \frac{\mathbf{v}^\dagger \mathbf{G}(\tilde{t}_\partial;\tilde{\gamma}_z)\mathbf{D}(\tilde{t}_{\Delta-\partial})\mathbf{G}^*(\tilde{t}_\partial;\tilde{\gamma}_z)\mathbf{v}}{\mathbf{v}^\dagger \mathbf{D}(\tilde{t}_{\Delta+\partial})\mathbf{v}} \tag{5}$$

As with the gpd model and the sgp model, there is only 1 free parameter in Eq. (5), *a*.

Eqs. (2), (3) and (5) are relevant only to a single emulsion droplet size, extraction of the droplet size distribution requires inversion of the attenuation data. On bench-top NMR apparatus this droplet size distribution is usually assumed to be a log-normal shape, inversion of the data is however possible using regularisation techniques [30]. The problem can be written in the form: **b** = **SP**, where **S** is a transfer matrix corresponding to the theoretical attenuation value for a given droplet radius, **b** is the acquired *I* data matrix and **P** is the droplet size distribution matrix which we are required to solve for. Normally a solution is obtained by finding **P** such that **H** is minimised:

$$\mathbf{H} = \min \|\mathbf{SP} - \mathbf{b}\|^2 \tag{6}$$

However **S** is generally ill-conditioned and unphysical fluctuations can be obtained. Applying regularisation, a penalty function is applied to penalise solutions of **P** containing unphysical oscillations. Hence, the solution equation is modified to the following form:

$$\mathbf{H} = \min(\|\mathbf{SP} - \mathbf{b}\|^2 + \lambda^2\|\mathbf{LP}\|^2) \tag{7}$$

The first term in Eq. (7), the residual, corresponds to how close **P** is to being a true solution to the physical problem. The second term in Eq. (7), the penalty function, controls the degree of smoothness of the function. **L** is the operator representing the choice of smoothness criterion, in our implementation this is the 2nd Derivative. λ is the regularisation parameter, controlling the degree of smoothness, which in our implementation we select based on the generalised cross validation (gcv) technique as described in [30], where further details regards the implementation of regularisation with respect to emulsion droplet sizing can be found.

3. Experimental

3.1. Magnet and spectrometer employed

The NMR system used for emulsion sizing experiments was a 25 mm gap 1.1 T 20 kg horse-shoe shaped permanent NdFeB magnet (corresponding to 47.7 MHz for detection of ^{1}H signal) and spectrometer, originally supplied from MR Technology, Japan and assembled by ABQMR, USA. Temperature control of the magnet was achieved using heating coils embedded within the magnet casing. This was supplemented by thermal insulation to minimise temperature and hence frequency drift. A photo of the assembled magnet is shown in Fig. 1a. The tightly wound solenoid rf micro-coils used to probe the emulsions were provided by ABQMR, USA. A photo of an assembled micro-coil is shown in Fig. 1b. They were available in a range of sizes (0.1–5 mm inner diameter) and feature either permanent or detachable flow inserts (using Upchurch connections, as shown in Fig. 1b) to enable, with respect to the experiments presented here, ease of sample loading (i.e. the emulsion could be slowly but readily pumped into the coil region). Further details with respect to the coils construction and performance can be sourced from McDowell and Adolphi [31] and McDowell and Fukushima [32]. The small sample volume prevents excessive magnet field heterogeneity from preventing chemical shift resolution of the oil and water phases. The magnet was also fitted with a 3D gradient system allowing a maximum gradient strength of 130 G/cm in the coil axis direction in which all diffusion measurements were made. This maximum gradient strength will place a limit on the range of oils that can be considered in terms of oil/water emulsions (as dictated by the T_1 and D_0 values for the respective oil and as discussed above). No such limitations exist for water/oil emulsions.

3.2. Emulsion systems studied

Three emulsions were prepared with decane (o/w), toluene (o/w) and crude oil (w/o) as the non-aqueous phase; these are hereafter referred to as Emulsions A, B and C. Their compositions are presented in Table 1, also shown is the value of *D* for the droplet phase as required by Eqs. (2), (3) and (5). All chemicals were obtained from Sigma Aldrich at purity >99%, except for middle-east light crude, supplied courtesy of Schlumberger Research, Cambridge. Emulsion preparation was performed using an ART MICCRA model high-shear mixer at 50 rpm for 10 min. A conductivity meter was used to confirm which liquid had formed the continuous phase.

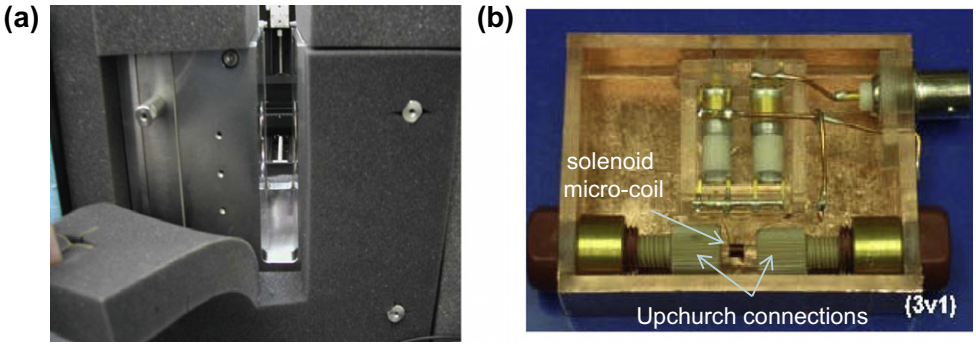

Fig. 1. (a) 1.1 T NdFeB permanent magnet used for droplet sizing experiments, including bespoke insulation used to minimise temperature fluctuation during data acquisition. (b) Interior of a 2 mm capillary rf micro-coil module used for excitation and signal detection. The micro-coil is connected to plastic tubing by Upchurch connections allowing samples to be readily pumped into the coil.

Table 1
Composition of emulsions.

	Droplet phase	Bulk phase	Emulsion type	Surfactant	Droplet phase D (m^2/s)
A	50 wt% decane	50 wt% water	o/w	2 vol% Tween 80 in aqueous phase	1.20×10^{-9}
B	50 wt% toluene	50 wt% water	o/w	2 vol% Tween 80 in aqueous phase	1.31×10^{-9}
C	25 wt% water	75 wt% middle-east light crude	w/o	None	2.41×10^{-9}

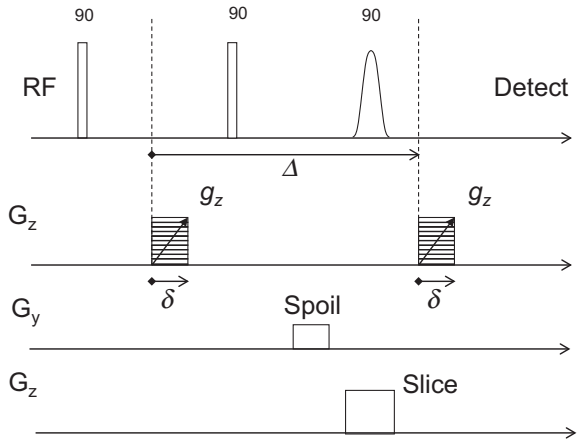

Fig. 2. PGSTE sequence used for droplet sizing measurements. Of note is the soft 90° pulse and slice gradient used to improve the homogeneity of the excited region, and hence reduce the peak line-widths.

3.3. Pulse sequence and data analysis employed

Droplet-sizing experiments were performed using a chemically resolved Pulsed Field Gradient (PFG) NMR sequence which employed a stimulated echo and slice selection along the flow direction (z). The pulse sequence is shown in Fig. 2. Selection of the micro-coil inner diameter for a particular emulsion proceeded as follows; the diameter of the micro-coil used and the width of the slice selection were increased until:

- sufficient chemical shift resolution was just retained such that differentiation of the oil and water phase peaks in a chemical spectrum was possible;
- a sufficient SNR (which was empirically determined to be in excess of 10 following signal averaging and 3 for a single acquisition) existed at the strongest gradient employed to enable peak identification for the droplet phase without signal averaging (see later) and
- an excessively high pressure drop (and hence difficulty with sample loading was experienced) during flow into the coil, due to emulsion viscosity, was avoided.

Consequently experiments on Emulsions A and B (toluene-in-water and decane-in-water emulsions) were performed using a 1 mm inner diameter rf coil and experiments on Emulsion C (water-in-crude-oil emulsions) employed a 5 mm inner diameter rf coil. The experimental parameters used for each sample is summarised in Table 2.

For all acquisitions, we acquired 2048 complex points in the time domain. These were Fourier transformed into the frequency-domain (without zero-filling, hence 2048 complex points in the frequency domain) for each time-domain acquisition. Corrections for frequency drift due to temperature variations within the magnet [33] were subsequently applied; hence requirement (ii) above. Signal averaging was thus performed in the frequency-domain. The chemical shift peak/s corresponding to the droplet phase was then extracted, its area determined as a function of gradient strength (g) and regularisation performed using the bgp method (Eq. (5)) to produce a droplet size distribution.

For verification purposes, optical microscopy was used to independently determine the droplet size distribution for Emulsions A and B using a Morphologi G3 instrument (Malvern, UK) [34]. 2 ml emulsion samples (these did not require dilution) were placed in a wet dispersion cell, they were then photographed using a 50X magnification (resulting in a 1.0 μm resolution). Image analysis, as provided by Malvern, was used to produce images of individual droplets (following gating), for each droplet the area of the droplet (and hence its diameter) as well as its elongation and circularity were determined, and hence distributions of these parameters produced. The elongation and circularity distributions were firmly located on 0 and 1 respectively, indicating that the droplets were not distorted. This procedure was fully automated. This enabled a total sample size of 20,321 droplets (Emulsion A) and 18,349 droplets to be analysed (Emulsion B); this sample size was validated against a total sample size of approximately half (12,301 and 11,990 droplets respectively) with no detectable change in the droplet size distribution produced. Such analysis was not successful for Emulsion C given the opaque nature of the crude oil employed.

4. Results and discussion

4.1. Validation of bgp method

In order to demonstrate the improved accuracy of the bgp method we conducted random walk simulations confined to a spherical droplet of diameter, a, and generated attenuation plots of the predicted measured signal against gradient strength or **q** (the random walk algorithm is based on that of [35,36]). Such a validation procedure is commonly employed for the validation of restricted diffusion models (e.g. [35]). The predictions of the gpd, sgp and bgp methods (Eqs. (2), (3) and (5) respectively) are plotted in non-dimensional form against this simulated data in Fig. 3a and b for two sets of conditions. For both, $\Delta/\delta = 10$; in (a) $\tilde{t}_\delta = \frac{D_0\delta}{a^2} = 0.05$, and in (b), $\tilde{t}_\delta = \frac{D_0\delta}{a^2} = 0.50$. The improved agreement of the bgp method with the simulated data, relative to the more conventionally used gpd and sgp methods, is clearly evident in both plots. In (a) for both the sgp and gpd method the resultant

Table 2
Experiment acquisition parameters for each emulsion.

	# Averages	Slice width (mm)	δ (ms)	Δ (ms)	# Grad. steps	Dwell time (μs)	Min./max. grad. (G/cm)	I/I_0 (max. grad.)	SNR (max. grad.)
A	4	3	3	230	16	200	0/84.7	0.041	33.34
B	8	2	5	250	32	200	0/62	0.051	26.31
C	16	2	2	100	32	100	0/113.2	0.013	14.58

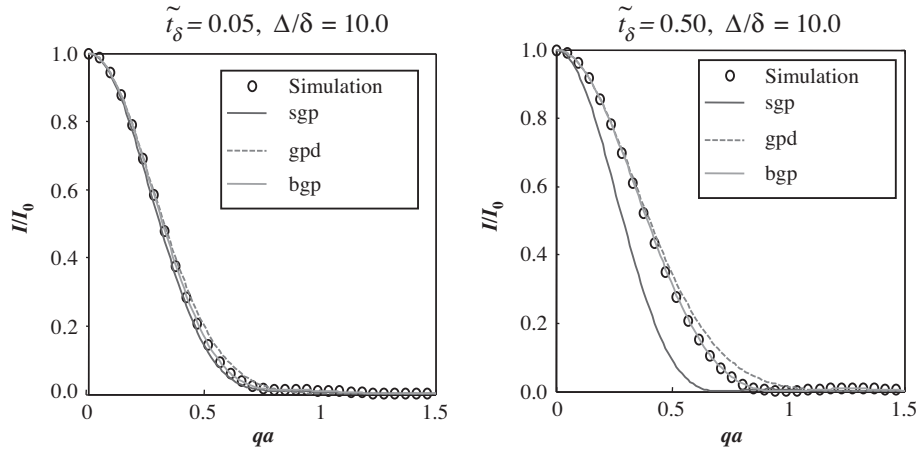

Fig. 3. Showing the effectiveness of the bgp algorithm in comparison to other methods (sgp and gpd) for simulated droplet size data where $\Delta/\delta = 10$ and (a) $\tilde{t}_\delta = \frac{D_0\delta}{a^2} = 0.05$, and (b), $\tilde{t}_\delta = \frac{D_0\delta}{a^2} = 0.50$.

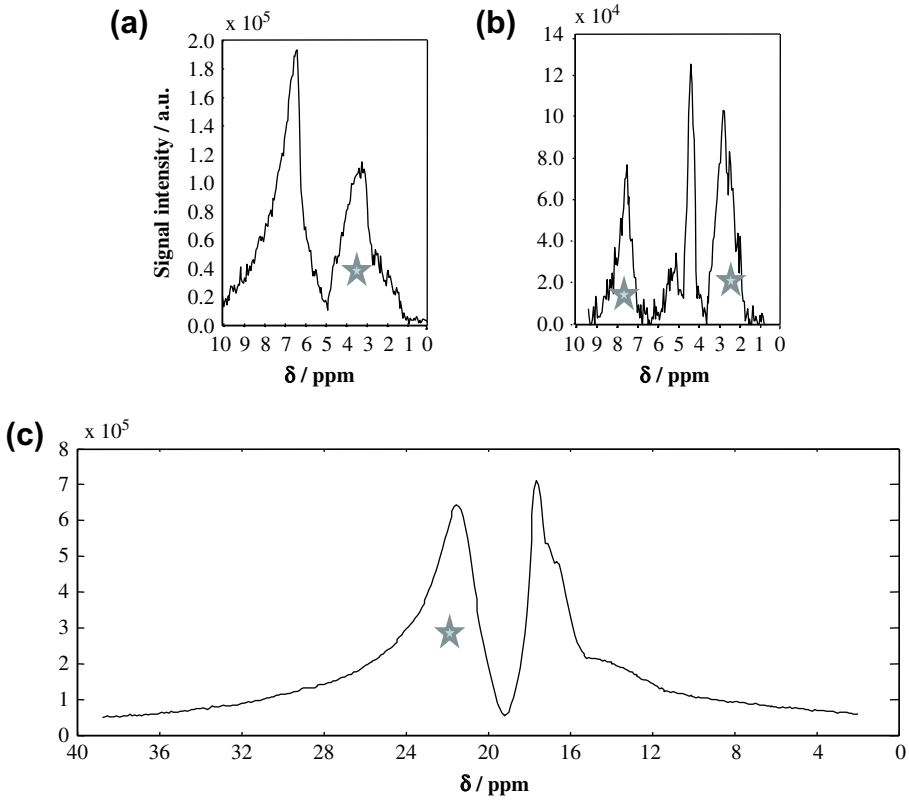

Fig. 4. Spectra obtained in the presence of an applied gradient showing chemical shift resolution and peak separation in three emulsions. (a) Emulsion A (Decane-in-water) – 42.36 G/cm. (b) Emulsion B (Toluene-in-water) – 31 G/cm. (c) Emulsion C (water-in-crude oil) – 14.15 G/cm. Stars indicate the peak corresponding to the droplet phase used in droplet sizing.

error in a (when treated as a free parameter) was 2%; for (b) the corresponding error in a was 12% for the sgp method and 4% for the gpd method. The error in a for the bpg method was less than 0.1% for both (a) and (b). This greater accuracy for the bpg method (which never exceeded 0.4% error in a) is consistently the case for all of the two-dimensional experimental parameter space (Δ/δ ranging from 1 to 20, $\tilde{t}_\delta = \frac{D_0\delta}{a^2}$ ranging from 0.01 to 0.1) that we have explored. In all simulations I/I_0 was allowed to attenuate (via appropriate adjustment of the **q** range) to approximately 0.01 with determination of 32 points.

4.2. Chemical shift resolution

The method described was able to produce spectra in which complete chemical shift resolution was obtained. This is shown for Emulsions A–C in Fig. 4, as produced by a single acquisition in the presence of an imposed set of gradients. Note that the requirement imposed in our methodology ((i) above) was that definitive peaks for the oil and water be evident – i.e. that the minima between peaks be adjacent to the noise level. Hence the spectral shapes are poor by spectrometry standards but provide

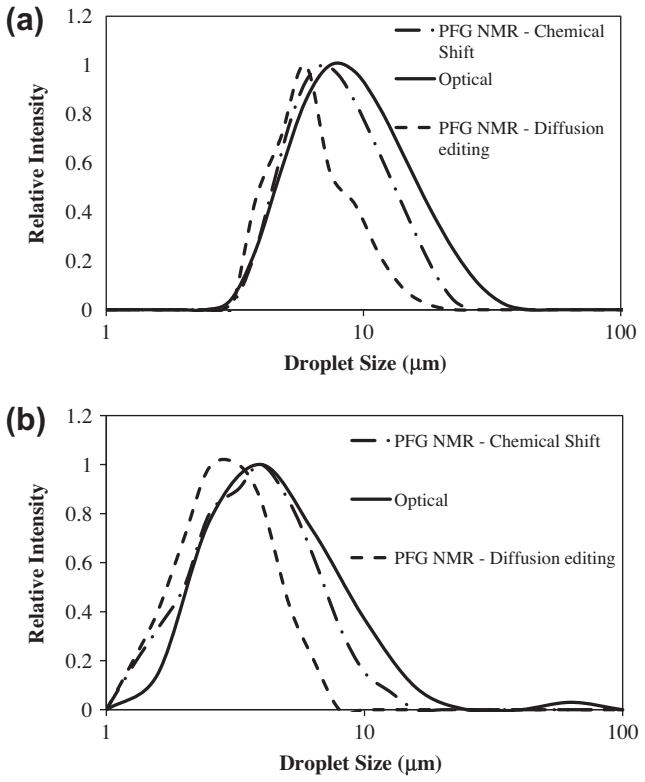

Fig. 5. Droplet size distributions obtained by PFG NMR on the 1.1 T system with bgp regularisation, compared with optical counting measurements for (a) Emulsion A (decane-in-water) emulsion and (b) Emulsion B (toluene-in-water).

Table 3
Emulsion droplet size distribution statistics.

Emulsion	Measurement method	$D_{3,2}$ (μm)	σ (μm)
A	Optical	8.7	12
A	NMR – Chemical shift	8.2	10.1
A	NMR – diffusion editing	5.7	6.4
B	Optical	4.8	6.3
B	NMR – Chemical shift	4.1	5.2
B	NMR – diffusion editing	3.2	4.3

sufficient resolution for peak area differentiation whilst maximising the available SNR by maximising the sample volume providing signal.

4.3. Droplet size distributions

The droplet size distribution acquired using PFG NMR and chemical shift phase differentiation is compared to that given by standard optical measurements where possible. Fig. 5 shows the comparison of distributions for (a) toluene-in-water (Emulsion A) and (b) decane-in-water (Emulsion B) emulsions. Also shown in Fig. 5a and b are the droplet size distributions produced for Emulsions A and B when the conventional approach of using diffusion editing to eliminate the water signal is employed. Table 3 presents the mean diameter ($D_{3,2}$) and the standard deviation (σ) of the distributions for Emulsions A and B and the three measurement techniques. What is immediately obvious in Fig. 5, backed up by the statistical data in Table 3, is that there is significantly better agreement between the chemical shift NMR data and the optical data. With reference to Table 1, where the diffusion coefficient of the (droplet) oil phase is presented, for the oils selected there is a relatively small difference between the oil diffusion coefficient and that of the continuous water phase. We speculate that this is the reason for the 'apparent' disappearance of the larger droplets from the droplet size distribution produced for both emulsions using diffusion editing to remove the water signal. Even in the case where there is a greater discrepancy between the respective D values for the oil and water phases, it is still difficult to determine that the water contribution to the acquired signal has been completely removed, particularly when it is experiencing restricted diffusion between the droplets.

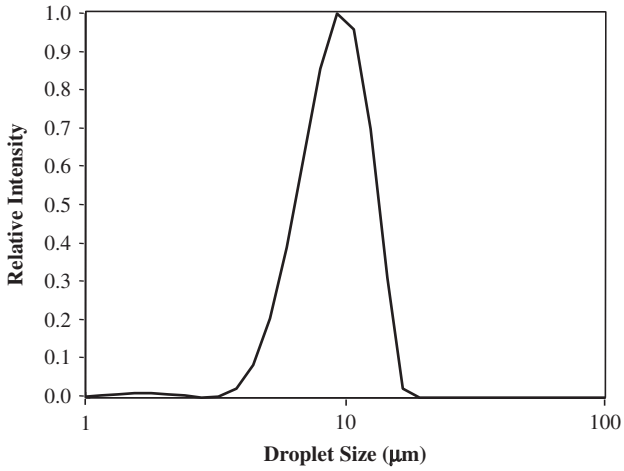

Fig. 6. Droplet size distribution obtained by PFG NMR for Emulsion C (water-in-crude oil).

The much smaller discrepancies between the Chemical Shift NMR and optical data can be attributed to various sources: sample selection and preparation for optical microscopy, shape registration during optical analysis (i.e. compression in the vertical direction, definition of internal boundary), size dependant relaxation during NMR analysis and temperature variations during NMR detection (recall sample volumes are relatively small and hence susceptible to temperature fluctuations). The last of these effects will be considered in more detail below.

Fig. 6 shows the droplet size distribution obtained for Emulsion C, water-in-crude oil ($D_{3,2}$ of 8.9 μm and σ of 5.1 μm). Attempts to make this measurement using NMR and T_1 nulling (as is conventionally practiced) to remove the continuous oil signal were not possible given the wide distribution (over an order of magnitude) of T_1 values present in the crude oil. The results obtained for the water-in-crude-oil emulsion show the possibility of using benchtop NMR for droplet sizing of opaque crude oil based systems with unambiguous detection of the water droplet phase signal.

4.4. Sensitivity analysis

In addition to causing frequency fluctuations due to very subtle temperature changes in the magnet, temperature changes in the sample will cause a change in the value of D and hence be a source of error in the determined emulsion droplet size distribution. In order to assess the impact of this effect, the droplet size distribution for the crude oil emulsion was predicted based on the bgp model (Eq. (5)) over a range of D corresponding to a temperature range of 15–25 °C as determined by O'Reilly and Peterson [37] (this can be considered a suitable range for application in typical industrial environments). Fig. 7 shows the change in droplet size distribution as a function of temperature. The results show that there is

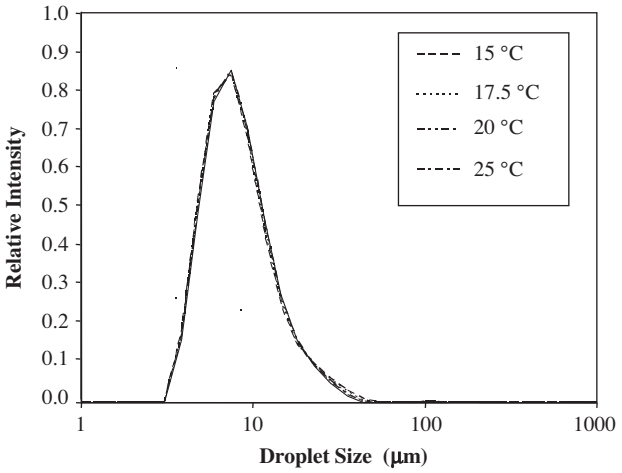

Fig. 7. Sensitivity analysis performed on Emulsion B (toluene-in-water), showing the droplet size distribution produced by the bgp method for temperatures between 15 °C and 25 °C and subsequent changes in D_0 for toluene.

negligible influence of temperature on the droplet size distribution produced by the bgp model over this temperature range.

5. Conclusions

It has been shown that a 1.1 T bench-top permanent magnet system can be used, with the aid of rf micro-coils, to obtain sufficient chemical shift resolution such that emulsion droplet sizing is possible with unambiguous determination of the droplet phase signal. A simple methodology which maximises the sample volume for SNR purposes whilst also ensuring that it is small enough such that magnetic field inhomogeneities do not prevent chemical shift resolution was implemented. This procedure is demonstrated on two model oil-in-water emulsions with results validated against optical microscopy. It is also demonstrated in a water-in-crude oil emulsion, a system with industrial relevance and for which there are no alternatives for emulsion droplet sizing. It has also been demonstrated that the bgp method of Barzykin [29] and Grebenkov [21–23] for analysing restricted self-diffusion in spheres improves accuracy relative to the more conventionally used sgp and gpd methods as are employed on commercial spectrometers for droplet sizing. Future work will focus on speeding up acquisition via the application of the Difftrain pulse sequence [38] which has been successfully demonstrated for emulsion droplet sizing on high field NMR spectrometers [39] and the use of alternative smaller magnets [33,40,41].

Acknowledgments

Funding is acknowledged from both Procter and Gamble (Newcastle, UK) and the EPSRC for IAL, and Microsoft Cambridge Research for equipment funding. Dr. Jon Mitchell (Schlumberger UK, University of Cambridge) is acknowledged for the provision of the crude oil sample. ABQMR (Eiichi Fukushima, Andrew McDowell) and MR Technology (Tomoyuki Haishi) are acknowledged for the NMR hardware provision and accompanying technical support.

References

[1] M.A. Voda, J. van Duynhoven, Characterization of food emulsions by PFG NMR, Trends. Food Sci. Tech. 20 (2009) 533–543.
[2] B. Balinov, O. Urdahl, O. Söderman, J. Sjöblom, Characterization of water-in-crude oil emulsions by the NMR self-diffusion technique, Colloid Surface A 82 (1994) 173–181.
[3] C.T. Verrips, J. Zaalberg, The intrinsic microbial stability of water-in-oil emulsions I. Theory, Eur. J. Appl. Microbiol. 10 (1980) 187–196.
[4] R. Pal, Effect of droplet size on rheology of emulsions, AICHE J. 42 (1996) 3181–3190.
[5] C.K. Reiffers-Magnani, J.L. Cuq, H.J. Watzke, Composite structure formation in whey protein stabilised o/w emulsions I. Influence of the dispersed phase on viscoelastic properties, Food Hydrocolloids 13 (1999) 303–316.
[6] D.J. McClements, Critical review of techniques and methodologies for characterization of emulsion stability, Crit. Rev. Food Sci. Nutr. 47 (2007) 611–649.
[7] J.E. Tanner, E.O. Stejskal, Restricted self-diffusion of protons in colloidal systems by the pulsed-gradient, spin-echo method, J. Chem. Phys. 49 (1968) 1768–1777.
[8] J.S. Murday, R.M. Cotts, Self-diffusion coefficient of liquid lithium, The J. Chem. Phys. 48 (1968) 4938–4945.
[9] K.J. Packer, C. Rees, Pulsed NMR studies of restricted diffusion. I. Droplet size distributions in emulsions, J. Colloid Interface Sci. 40 (1972) 206–218.
[10] M.L. Johns, K.G. Hollingsworth, Characterisation of emulsion systems using NMR and MRI, Prog. Nucl. Mag. Reson. Spectrosc. 50 (2007) 51–70.
[11] M.L. Johns, NMR studies of emulsions, Current Opin. Colloid Interface Sci. 14 (2009) 178–183.
[12] I. Fourel, J.P. Guillement, D. Le Botlan, Determination of water droplet size distributions by low resolution PFG-NMR II. "Solid" emulsions, J. Colloid Interface Sci. 169 (1995) 119–124.
[13] J.C. Van den Eden, D. Waddington, H. Van Aalst, C.G. Van Kralingen, K.J. Packer, Rapid determination of water droplet size distributions by PFG-NMR, J. Colloid Interface Sci. 140 (1990) 105.
[14] G.J.W. Goudappel, J.P.M. van Duynhoven, M.M.W. Mooren, Measurement of oil droplet size distributions in food oil/water emulsions by time domain pulsed field gradient NMR, J. Colloid Interface Sci. 239 (2001) 535–542.
[15] P.S. Denkova, S. Tcholakova, N.D. Denkova, K.D. Danov, B. Campbell, C. Shawl, D. Kim, Evaluation of the precision of drop-size determination in oil/water emulsions by low resolution NMR spectroscopy, Langmuir 20 (2004) 11402–11413.
[16] J.P.M. van Duynhoven, G.J.W. Goudappel, G. van Dalen, P.C. van Bruggen, J.C.G. Blonk, A.P.A. M Eijkelenboom, Scope of droplet size measurements in food emulsions by pulsed field gradient NMR at low field, Mag. Reson. Chem. 40 (2002) S51–S59.
[17] A. Pena, G.J. Hirsaki, Enhanced characterization of oilfield emulsions via NMR diffusion and transverse relaxation experiments, Adv. Colloid Interface Sci. 105 (2003) 103–150.
[18] A. Bot, F.P. Duval, W.G. Bouwman, Effect of processing on droplet cluster structure in emulsion gels, Food Hydrocolloids 21 (2007) 844–854.
[19] J. van Duynhoven, A. Voda, M. Witek, H. Van As, Chapter 3 – Time-Domain NMR Applied to Food Products, Annual Reports of NMR Spectroscopy 69 (2010) 145–197.
[20] L. Grunin, B. Blümich, Resolving chemical shift spectra with a low-field NMR relaxometer, Chem. Phys. Lett. 397 (2004) 306–308.
[21] D.S. Grebenkov, NMR Survey of reflected Brownian motion, Rev. Modern Phys. 79 (2007) 1077–1137.
[22] D.S. Grebenkov, Laplacian eigenfunctions in NMR. I. A numerical tool, Concepts Mag. Reson. A 32A (2008) 277–301.
[23] D.S. Grebenkov, Laplacian eigenfunctions in NMR. II. Theoretical advances, Concepts Mag. Reson. A 34A (2009) 264–296.
[24] E.O. Stejskal, J.E. Tanner, Spin diffusion measurements: spin echoes in the presence of a time-dependent field gradient, J. Chem. Phys. 42 (1965) 288–292.
[25] A. Caprihan, L.Z. Wang, E. Fukushima, A multiple-narrow-pulse approximation for restricted diffusion in a time-varying field gradient, J. Magn. Reson. 118 (1996) 94–102.
[26] P.T. Callaghan, A simple matrix formalism for spin echo analysis of restricted diffusion under generalized gradient waveforms, J. Magn. Reson. 129 (1997) 74–84.
[27] B.N. Ryland, P.T. Callaghan, Spin echo analysis of restricted diffusion under generalized gradient waveforms for spherical pores with relaxivity and interconnections, Israel J. Chem. 43 (2003) 1–7.
[28] H.C. Torrey, Bloch equations with diffusion terms, Phys. Rev. 104 (1956) 563.
[29] A.V. Barzykin, Theory of spin echo in restricted geometries under a step-wise gradient pulse sequence, J. Magn. Reson. 139 (1999) 342–353.
[30] K.G. Hollingsworth, M.L. Johns, Measurement of emulsion droplet sizes using PFG NMR and regularization methods, J. Colloid Interface Sci. 258 (2003) 383–389.
[31] A.F. McDowell, N.L. Adolphi, Operating nanoliter scale NMR microcoils in a 1 tesla field, J. Magn. Reson. 188 (2007) 74–82.
[32] A.F. McDowell, E. Fukushima, Ultracompact NMR: ^{1}H spectroscopy in a subkilogram magnet, Appl. Mag. Reson. 35 (2008) 185–195.
[33] B. Blümich, F. Casanova, S. Appelt, NMR at low magnetic fields, Chem. Phys. Lett. 477 (2009) 231–240.
[34] http://www.malvern.com/labeng/products/morphologi/particle_image_analyzer.htm.
[35] B. Balinov, B. Jönsson, P. Linse, O. Söderman, The NMR self-diffusion method applied to restricted diffusion. Simulation of echo attenuation from molecules in spheres and between planes, J. Magn. Reson. 104 (1993) 17–25.

[36] B. Manz, L.F. Gladden, P.B. Warren, Flow and dispersion in porous media: lattice-Boltzmann and NMR studies, ALCHE J. 45 (1999) 1845–1854.
[37] D.E. O'Reilly, E.M. Peterson, Self-diffusion coefficients and rotational correlation times in polar liquids. III. Toluene, J. Chem. Phys. 56 (1972) 2262–2266.
[38] J.P. Stamps, B. Ottink, J.M. Visser, J.P.M. van Duynhoven, R. Hulst, Difftrain: a novel approach to a true spectroscopic single-scan diffusion measurement, J. Magn. Reson. 151 (2001) 28–31.
[39] K.G. Hollingsworth, A.J. Sederman, C. Buckley, L.F. Gladden, M.L. Johns, Fast emulsion droplet sizing using NMR self-diffusion measurements, J. Colloid Interface Sci. 274 (2004) 244–250.
[40] E. Danieli, J. Mauler, J. Perlo, B. Blümich, F. Casanova, Mobile sensor for high resolution NMR spectroscopy and imaging, J. Magn. Reson. 198 (2009) 80–87.
[41] E. Danieli, J. Mauler, J. Perlo, B. Blumich, F. Casanova, Small magnets for portable NMR spectrometers, Angew. Chem. Int. Ed. 49 (2010) 4133–4135.